Bioresource Technology 241 (2017) 1145–1151

Contents lists available at ScienceDirect

Bioresource Technology

journal homepage: www.elsevier.com/locate/biortech

Short Communication

Greenhouse gas emissions and the links to plant performance in a fixed-film activated sludge membrane bioreactor – Pilot plant experimental evidence

Giorgio Mannina [a], Marco Capodici [a], Alida Cosenza [a], Daniele Di Trapani [a,*], Gustaf Olsson [b]

[a] Dipartimento di Ingegneria Civile, Ambientale, Aerospaziale, dei Materiali, Università di Palermo, Viale delle Scienze, Ed. 8, 90128 Palermo, Italy
[b] Department of Industrial Electrical Engineering and Automation (IEA), Lund University, Box 118, SE-22100Ole Römers väg 1, Lund, Sweden

HIGHLIGHTS

- A constitutive relationship among OCs, EQI, EF and GHG emissions was found.
- Increase of air flow led to a decrease of the EQI, increasing indirect emissions.
- Direct emissions increase with the air flow rate due to higher N_2O production.
- High air flow rates increase the contribution of the MBR tank in producing N_2O.

GRAPHICAL ABSTRACT

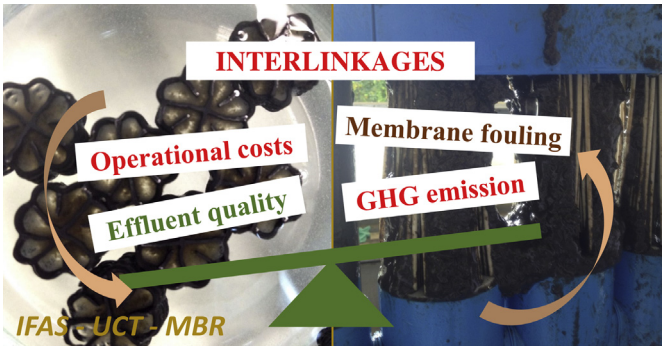

ARTICLE INFO

Article history:
Received 7 March 2017
Received in revised form 5 May 2017
Accepted 7 May 2017
Available online 18 May 2017

Keywords:
Wastewater treatment
Membrane bioreactor
Moving bed biofilm reactor
Greenhouse gas emission
Mathematical modelling

ABSTRACT

The present study explores the interlinkages among the operational variables of a University of Cape Town (UCT) Integrated Fixed Film Activated Sludge (IFAS) membrane bioreactor (MBR) pilot plant. Specifically, dedicated experimental tests were carried out with the final aim to find-out a constitutive relationship among operational costs (OCs), effluent quality index (EQI), effluent fines (EF). Greenhouse gas (GHG) emissions were also included in the study. Results showed that the EQI increases at low flow rate likely due to the dissolved oxygen (DO) limitation in the biological processes. Direct GHGs increase with the increasing of the air flow due to the anoxic N_2O contribution. Irreversible membrane fouling reduce from 98% to 85% at the air flow rate of 0.57 $m^3\ h^{-1}$ and 2.56 $m^3\ h^{-1}$, respectively. However, the increase of the air flow rate leads to the increase of the N_2O–N flux emitted from the MBR (from 40% to 80%).

1. Introduction

Stringent effluent limits and the need of a higher environment protection have pushed towards more advanced technologies for wastewater treatment (Mannina and Viviani, 2009). Among these the performance of membrane bioreactors (MBRs) and moving bed biofilm reactors (MBBRs) have been thoroughly analysed in the past years and have demonstrated several advantages compared to conventional treatment methods (Ødegaard, 2006; Judd, 2011). Recently, the combination of MBR and MBBR in the Integrated Fixed Film Activated Sludge (IFAS) configuration has been proposed with the aim to further improve the treatment efficiency (Mannina et al., 2017a). During the last few years, the environmen-

* Corresponding author.
E-mail address: daniele.ditrapani@unipa.it (D. Di Trapani).

http://dx.doi.org/10.1016/j.biortech.2017.05.043
0960-8524/

tal impacts associated with the wastewater treatment have been broadened and the "air" has been included as new target together with the "water" and "soil" (Flores-Alsina et al., 2014). It has already recognized that wastewater treatment can result in direct emissions of greenhouse gases (GHGs) such as carbon dioxide (CO_2), methane (CH_4) and nitrous oxide (N_2O), mainly due to the biological processes (Gupta and Singh, 2012; Massara et al., 2017). WWTPs are also responsible for indirect emissions related to power generation, chemicals manufacturing and sludge disposal (Fine and Hadas, 2012; Flores-Alsina et al., 2014; Mannina et al., 2016a). Therefore, GHGs emissions have to be considered, in addition to effluent quality and operational costs, when comparing design alternatives or operation scenarios (Guo et al., 2016). The identification of the interrelationship between operational conditions and GHG emissions represents a key issue in view of reducing the GHG emissions by maintaining feasible operational costs and good effluent quality. However, there are only few studies that have explored the N_2O emission from advanced technologies based on biofilm growth (Todt and Dörsch, 2016; Mannina et al., 2017a; Sabba et al., 2017).

Bearing in mind the above considerations, the novelty of this study is based on the evaluation of direct and indirect GHG emissions as well as operational costs (OCs) and effluent quality index (EQI) in a University of Cape Town (UCT) IFAS-MBR pilot plant. The objectives of the study are: i. Quantify the effect of the air flow variation, required for membrane fouling mitigation, on EQI, OC and GHG emission; ii. Gain insights in view of proposing a quantitative interrelationship among OCs, EQI and GHG.

The authors hope that the results of the study will be useful in the development of a conceptual mathematical tool to support decision-makers and plant managers to design, operate, and manage MBR WWTPs causing less operational costs and environmental impacts, both in terms of liquid and air emissions.

2. Materials and methods

The pilot plant and the sampling campaign are described in Section 2.1. Membrane fouling is a critical part of the operation and is assessed in Section 2.2. Then, performance indicators are defined in Section 2.3 and aeration demand is finally described in Section 2.4.

2.1. Description of the pilot plant and sampling campaign

A UCT-IFAS-MBR pilot plant has been designed and set up at the Laboratory of Sanitary and Environmental Engineering of Palermo University (Mannina et al., 2017a). The pilot plant consists of one anaerobic (volume 62 L), one anoxic (volume 102 L) and one aerobic (volume 211 L) tank according to the UCT scheme. Suspended carriers (courtesy of Amitec s.r.l.) were added in the anoxic and aerobic tanks for biofilm growth. The filling ratios are 15% and 40% in the anoxic and aerobic reactor, respectively. The solid-liquid separation is carried out by means of an ultrafiltration hollow fiber membrane module (PURON® 3 bundle, porosity: 0.03 μm, surface: 1.4 m^2, courtesy of Koch Membrane Systems, Inc.). The membrane module is located inside a dedicated aerated compartment (MBR tank) (36 L). The membrane has been periodically backwashed (every 9 min for a period of 1 min) by pumping a volume of permeate from the Clean In Place (CIP) tank. The extraction flow rate was set equal to 20 L h^{-1} (Q_{OUT}) through the membrane module. Each tank is equipped with a specific cover that enables to capture the N_2O produced from each tank as well as from the entire pilot plant.

The pilot plant was operated at 30 days of sludge retention time (SRT) and was fed with municipal wastewater mixed with a synthetic wastewater characterized by Sodium Acetate (CH_3COONa), glycerol ($C_3H_8O_3$), dipotassium hydrogen phosphate (K_2HPO_4). The UCT-IFAS-MBR pilot plant was started up with sludge inoculum, withdrawn from the Municipal WWTP of Palermo. After 68 days start-up phase, the experimental campaign was divided into four phases each characterized by a different air flow rate in the MBR and aerobic compartments: Phase I, 0.57 m^3 h^{-1}; Phase II, 1.13 m^3 h^{-1}; Phase III, 1.70 m^3 h^{-1}; Phase IV, 2.26 m^3 h^{-1}. Each phase had a duration of one week during which a constant air flow rate (different for each Phase) was superimposed. In Table S1, provided as Supplementary material, the main influent and operational features are summarized.

During the pilot plant operations, the influent wastewater, the different reactors and the effluent permeate have been sampled and analysed for TSS, volatile suspended solids (VSS), total chemical oxygen demand (COD_{TOT}), supernatant filtered COD (COD_{SUP}), ammonium nitrogen (NH_4–N), nitrite nitrogen (NO_2–N), nitrate nitrogen (NO_3–N), total nitrogen (TN), phosphate (PO_4–P), total phosphorus (TP). All analyses have been carried out according to the Standard Methods (APHA, 2005). Liquid and gaseous samples were withdrawn from the anaerobic, anoxic, aerobic and MBR tanks and analysed to determine the N_2O–N concentration according to Mannina et al. (2016b, 2016c). Furthermore, the N_2O–N fluxes (gN_2O–N m^{-2} h^{-1}) from all compartments were quantified by measuring the gas flow rates, Q_{gas} (L min^{-1}) according to the procedure reported in Mannina et al. (2011, 2017b) and Di Trapani et al. (2010, 2014).

2.2. Membrane fouling assessments

Membrane fouling has been assessed by monitoring the total resistance (R_T) to filtration, during pilot plant ordinary operations, according to the general form of the Darcy's Law (Eq. (1)):

$$R_T = \frac{TMP}{\mu J} \quad (1)$$

where R_T is the resistance to filtration (m^{-1}), TMP is the transmembrane pressure (Pa), μ the permeate viscosity (Pa·s), and J the permeation flux (m s^{-1}).

R_T can be defined as the sum between the intrinsic resistance of membrane in tap water (R_m) and the resistance due to membrane fouling (R_F); the latter can be fractionated according to Eq. (2).

$$R_F = R_{PB} + R_{C,irr} + R_{C,rev} = R_T + R_m \quad (2)$$

where R_{PB} is the irreversible resistance due to colloids and particles deposition into the membrane pore; $R_{C,irr}$ is the fouling resistance related to superficial cake deposition that can be only removed by physical cleanings (hydraulic/sponge scrubbing); $R_{C,rev}$ is the fouling resistance related to superficial cake deposition that can be removed by ordinary backwashing.

The analysis of the specific fouling mechanisms was carried out through the application of the resistance-in-series (RIS) model based on cake layer removal with "extraordinary physical cleanings" (Di Bella et al., 2007; Mannina et al., 2017c). The superficial cake layer deposition was analysed by calculating a series of flux and transmembrane pressure (TMP) data before and after the cake layer removal from the membrane surface. The fouling resistance R_F can also be expressed as the sum of an irreversible resistance (R_{irr}), related to the pore blocking and cake deposition not removable by ordinary backwashing and a reversible contribution (R_{rev}), the latter consisting in the fouling amount removable through ordinary backwashing (Eq. (3)) (Di Bella et al., 2015).

$$R_F = R_{rev} + R_{irr} \quad (3)$$

where R_{rev} and R_{irr} have been previously defined.

According to the RIS model, through the membrane cleaning operations the reversible/irreversible mechanisms could be eviscerated.

Furthermore, the fouling rate (FR) [$m^{-1}\,d^{-1}$] was assessed according to Eq. (4).

$$FR = \frac{R_{T,(t+1)} - R_{T,(t)}}{\Delta t} \quad (4)$$

where $R_{T,(t+1)}$ and $R_{T,(t)}$ is the resistance at the time t + 1 and t, respectively.

At the beginning of each experimental phase, the membrane was subject to physical cleaning operations in order to compare the fouling tendency in the different phases.

2.3. Performance indicators

Direct emissions were evaluated as the total N_2O-N concentration in the liquid and gaseous samples withdrawn from each tank. More precisely, direct emissions were quantified in terms of both liquid and gaseous form. The total gaseous mass of N_2O-N measured was converted into mass of equivalent CO_2 per cubic meter of treated water ($gCO_2eq\,m^{-3}$) by adopting the global warming potential coefficient for N_2O (equal to 298 $gCO_2eq\,g^{-1}N_2O$) (IPCC, 2007) and the treated volume of wastewater per day. Similarly, the liquid direct emission was quantified by converting the mass of dissolved N_2O-N in the permeate into $gCO_2eq\,m^{-3}$.

To evaluate the indirect emissions (expressed as g of equivalent CO_2 per cubic meter of treated water), the energy required for the aeration, P_w [$kWh\,m^{-3}$], and for the permeate extraction, P_{eff} [$kWh\,m^{-3}$], was quantified. P_w and P_{eff} were converted into gCO_2-eq m^{-3} and € m^{-3} by means of two conversion factors: $\gamma_{power,GHG}$ [0.7 $gCO_2eq\,kWh^{-1}$] and γ_e [0.806 € kWh^{-1}], respectively (Mannina and Cosenza, 2015).

The effluent fine, EF [€ m^{-3}], was evaluated according to Eq. (5). For each relevant pollutant (j), the effluent concentration (C_{jEFF}) was compared with the imposed effluent limits ($C_{L,j}$) during the evaluation period (t_2-t_1).

$$EF = \frac{1}{t_2 - t_1} \cdot \int_{t_1}^{t_2} \left[\frac{1}{Q_{IN}} \cdot \left(\sum_{j=1}^{n} \left(\begin{array}{l} Q_{OUT} \cdot \Delta\alpha_j \cdot C_j^{EFF} + (Q_{OUT}) \cdot \\ \left[\beta_{0,j} + (C_j^{EFF} - C_{L,j}) \cdot (\Delta\beta_j - \Delta\alpha_j) \right] \end{array} \right) \right. \right.$$
$$\left. \left. \cdot (viside \cdot (C_j^{EFF} - C_{L,j})) \right) \right] \cdot dt \quad (5)$$

where Q_{IN} and Q_{OUT} are the influent and effluent flow, respectively; $\Delta\alpha_j$ is the slope of the curve EF versus C_{jEFF} when $C_{jEFF} < C_{L,j}$ (in this case, the function Heaviside = 0); $\Delta\beta_j$ represents the slope of the curve EF versus C_{jEFF} when $C_{jEFF} > C_{L,j}$ (in this case, the function Heaviside = 1); $\beta_{0,j}$ are the increment of the fines for the latter case.

Finally, the operational costs, OCs [€ m^{-3}], were calculated by adapting the cost function reported in Mannina and Cosenza (2015) (Eq. (6)); where EF includes N_2O.

$$OC = (P_w + P_{eff}) \cdot \gamma_e + EF \quad (6)$$

In this study, the concentration of COD_{TOT}, TN, PO_4-P and dissolved N_2O in the permeate (coupled with gaseous N_2O) were considered. The same C_{jEFF} value according to Stare et al. (2007) was considered for each pollutant. Concerning the N_2O, the value of C_{jEFF} deduced from Flores-Alsina et al. (2014) was adopted. For $C_{L,j}$ the emission limits mandated by Italian laws were adopted. Regarding the N_2O, no effluent limits were found in literature, therefore the same limit for PO_4-P was adopted.

The Effluent Quality Index, expressed as load of pollution unit (PU), EQI [$kgPU\,d^{-1}$], has been also adopted as performance indicator. The EQI represents the pollutant mass that is discharged throughout the evaluation period. Here the EQI was evaluated modifying the equation proposed by Mannina and Cosenza (2015). Specifically, the mass of N_2O discharged (both liquid and gaseous phase) was included by adopting a weighting factor for N_2O (both liquid and gaseous) equal to 100 (Eq. (7)).

$$EQI = \frac{1}{T \cdot 1000} \cdot \int_{to}^{t1} \left(\begin{array}{l} \beta_{COD} \cdot COD_{TOT} + \beta_{TN} \cdot TN + \beta_{PO} \cdot PO_4 - P + \\ \beta_{N2Ogas} \cdot N_2O_{gas} + \beta_{N2O,L} \cdot N_2O_L \end{array} \right) \cdot Q_{OUT} \cdot dt \quad (7)$$

where β_{COD}, β_{TN}, β_{PO}, β_{N2Ogas} and $\beta_{N2O,L}$ are the weighting factors of the effluent COD_{TOT}, TN, PO_4-P, liquid N_2O in the permeate and gaseous N_2O. The following weighting were adopted (Mannina and Cosenza, 2015): β_{COD} = 1, β_{TN} = 20, β_{PO} = 50. For the N_2O on the basis of the study of Flores-Alsina et al. (2014) the value of 100 was adopted both for β_{N2Ogas} and $\beta_{N2O,L}$.

2.4. Specific aeration demand

For each experimental phase the specific aeration demand (SAD) based on membrane (SAD_m) [$m^3\,m^{-2}\,h^{-1}$] and the specific aeration demand based on permeate volume (SAD_p) [$m^3\,m^{-3}$] were evaluated according to Eqs. (8) and (9), respectively.

$$SAD_m = \frac{Q_{air}}{A_m} \quad (8)$$

where Q_{air} [$m^3\,h^{-1}$] is the air flow rate and A_m [m^2] is the total membrane surface

$$SAD_p = \frac{Q_{air}}{J \cdot A_m} = \frac{Q_{air}}{Q_p} \quad (9)$$

where J [$m\,h^{-1}$] is permeate flux and Q_p [$m^3\,h^{-1}$] is permeate flow rate, whilst A_m and Q_{air} have been previously defined in Eq. (8).

3. Results and discussion

We first describe the results of direct and indirect emissions. In the following sections, the interlinkage between the air flow rates, EQI, EF, OC and the direct and indirect GHG emissions will be discussed in order to provide a groundwork required for the future setting up of the conceptual mathematical model able to connect the physical and biological processes in the GHG emissions.

3.1. Direct and indirect emission and performance indicators

The results of the indirect and direct emissions for each experimental phase as well as data related to the performance indicators (EF, EQI and OC) are summarized in Table S2, provided as Supplementary material. Furthermore, data related to the performance indicators (EF, EQI and OC) are reported in Table S2.

From the Table S2 it can be observed that indirect emissions are several orders of magnitude higher than the direct ones. This suggests that the power consumption is a primary contributor to the total GHG emission. However, particular operating conditions of the pilot plant can lead to a considerable increase of direct GHG emission. Indeed, the amount of direct GHG emitted from the pilot plant range between 0.006% and 0.6% of the total emission.

With the increase of the air flow rates (from Phase I to Phase IV) both direct and indirect GHG emissions increased (Table S2). Direct emissions increased likely due to a twofold reason: i. High DO concentration inside the anoxic tank, which promotes the N_2O production during the denitrification; ii. An increase of the stripping effect of the dissolved N_2O with the increase of the air flow. During Phase III the amount of influent ammonia (average value of 75 $mg\,L^{-1}$) was completely nitrified (average nitrification efficiency of 99%). However, due to the high DO concentration inside the anoxic tank (0.04 $mg\,L^{-1}$) only 25% (as average value) of the produced nitrate

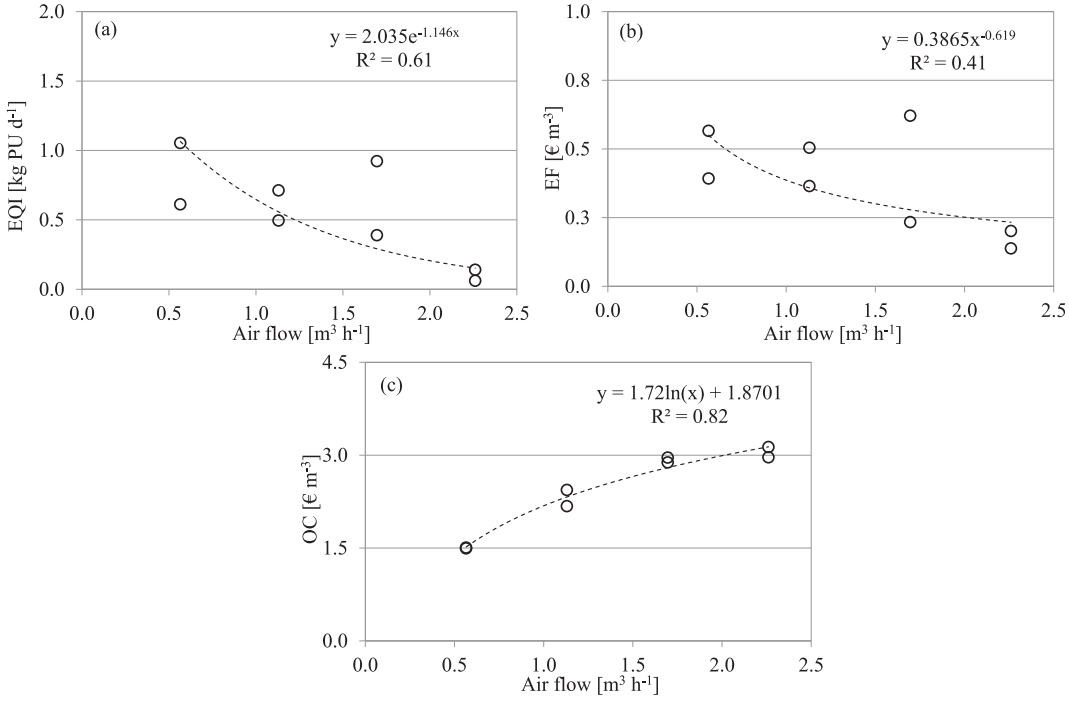

Fig. 1. Air flow versus (a) EQI, (b) EF and (c) OC.

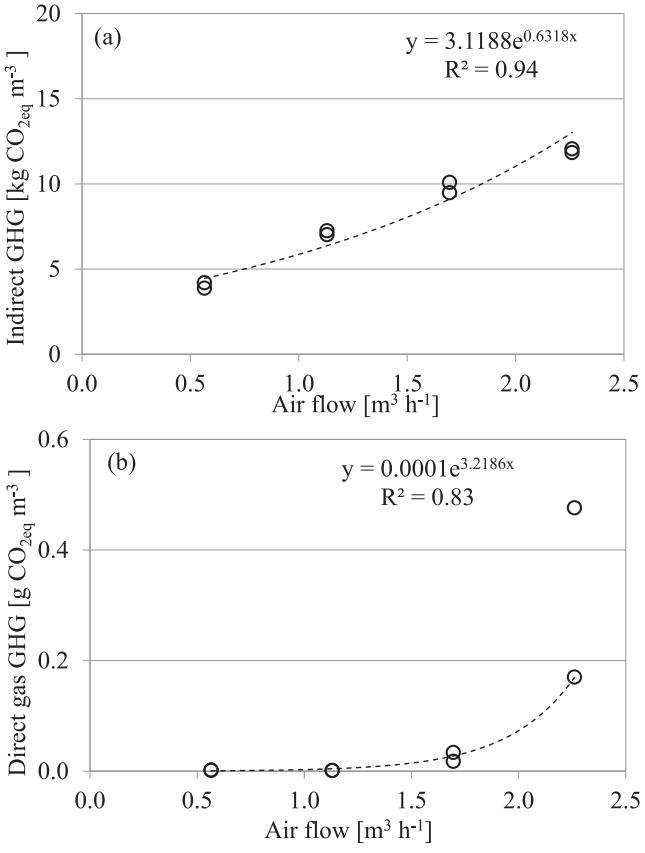

Fig. 2. Relationship between (a) air flow and indirect GHG emissions; (b) air flow rate and direct GHG emissions.

was denitrified. Therefore, a high amount of dissolved N_2O could accumulate in the anoxic tank (0.48 mg L^{-1}).

Both EF and EQI decreased during Phase IV mainly due to the complete nitrification and the decrease of the pollutants load discharged into environment (Table S2). The OCs were strongly influenced by the air flow rate increase, requiring more electric power. Indeed, with the increase of the air flow rate the OCs value increased mainly due to the greater amount of power required for the aeration. By quadrupling the air flow rate from Phase I to Phase IV, the OC value doubled from 1.5 € m^{-3} to 3.05 € m^{-3}, respectively.

3.2. Specific aeration demand

Table S3, provided as Supplementary material, summarizes the average SAD_m and the SAD_p values for each experimental phase. The table reveals that both SAD_m and SAD_p increased with the air flow rate. Typical SAD_m values range between 0.2 and 1.5 $m^3\ m^{-2}$ - h^{-1} while the value of SAD_p varies between 10 and 90 $m^3\ m^{-3}$ (Singh et al., 2006). The SAD_m and SAD_p depends on the type and operation of the MBR. The increase of SAD_m and SAD_p is likely because the pilot plant was operated at constant permeate flux.

3.3. Constitutive relations between the air flow rate and the performance measures

The correlations between the air flow rate and EQI (a), EF (b) and OC (c) are shown in Fig. 1. Fig. 1a shows that the EQI decreases with an increasing air flow rate. Still the relationship is not quantitatively certain, given the correlation coefficient value R^2 = 0.61.

The decrease of EQI with the increase of the air flow rate is mainly due to: i. The improvement of the biological processes (carbon removal and ammonia oxidation) with the increase of the DO inside the aerated tanks; ii. The decrease of N_2O produced during nitrification. It is proposed that during the oxygen limiting conditions, autotrophic ammonia oxidizers use nitrite as the terminal electron acceptor to save oxygen for the oxygenation reaction of ammonia to hydroxylamine thus contributing to the N_2O production during nitrification (Kampschreur et al., 2009). However, high aeration may also lead to an increased amount of DO recycled in the denitrification tank, which also may lead to the increase of N_2O emissions during denitrification (Kampschreur et al., 2009).

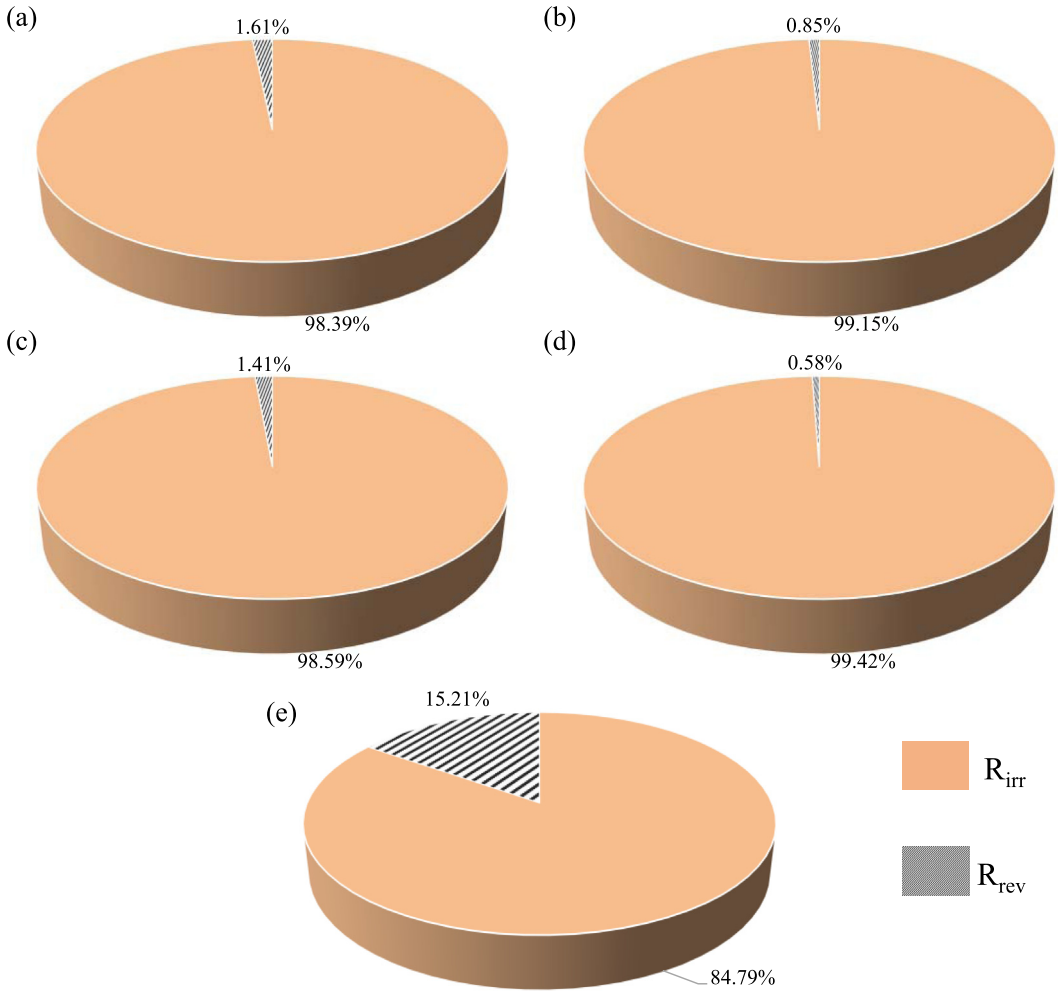

Fig. 3. Fouling fractionation according to the RIS method at the beginning of Phases I-IV (a–d) and at the end of the Phase IV (e).

The improvement of the biological processes at high air flow rates leads to a reduction of the mass of pollutants discharged in the environment with a consequent decrease of the fines to be paid (Fig. 1b). Therefore, in terms of both EQI and EF, the highest air flow rate (Phase IV) represents the best operating condition. However, high air flow rates lead to higher aeration power demand, thus increasing OC (Fig. 1c). The maximum OC value (3 € m^{-3}) appeared during Phase IV having the highest air flow. Thus, the outcome is logical that operating the plant at the highest air flow gives a better effluent quality at the expense of higher OCs.

3.4. Constitutive relations between the air flow rate, direct and indirect GHG emissions

In Fig. 2 data related to the relationship between the air flow versus indirect (a) and direct emissions (b) are displayed. The indirect GHG emissions are strongly influenced by the increase of the air flow rate (Fig. 2a). The relationship between the air flow rate and the direct GHG emissions can be modelled as an exponential relationship (R^2 = 0.83).

There is also an exponential relationship between air flow and direct emissions (Fig. 2b) and increasing air flow rate leads to higher direct emissions. As discussed above the great amount of DO introduced into the anoxic tank by means of the recycled sludge from the aerobic tank inhibits both synthesis and activity of denitrification enzymes leading to N_2O emission during denitrification (Otte et al., 1996). The latter consideration has essential importance for the air flow rate control: while high aerobic DO concentrations will reduce the amount of N_2O produced during nitrification, the N_2O produced during denitrification will increase.

The lowest air flow rate (Phase I) seems to be the most favourable condition with respect to GHG emissions (both direct and indirect). However, the EQI and EF have their highest values during Phase I. Consequently, the interlinkages between the different involved criteria require a "multiple trade-off" in order to identify the best value of the air flow rate for mitigation of GHG emissions while reducing at the same time the EQI and OCs values.

3.5. Membrane fouling and GHG emissions

The results of the application of the RIS model during the physical membrane cleanings operated at the beginning of Phases I-IV (a-d) and at the end of Phase IV (e) are displayed in Fig. 3.

The variation of the air flow rate (for fouling mitigation) strongly influenced the nature of membrane fouling as shown in Fig. 3. From Phase I (Fig. 3a) to the end of Phase IV (Fig. 3d) it was observed a substantial increase of the reversible resistance due to cake deposition (R_{rev}) (from 1.6% to 15%). This result is likely due to the increased scouring effect of the high air flow rate (during Phase IV) that makes the cake layer less compact thus enabling its detachment during the backwashing. Therefore, since the minimum value of the irreversible resistance R_{irr} (85%) was obtained by adopting the highest air flow rate (Phase IV), the operating conditions related to Phase IV represent the best way to manage the

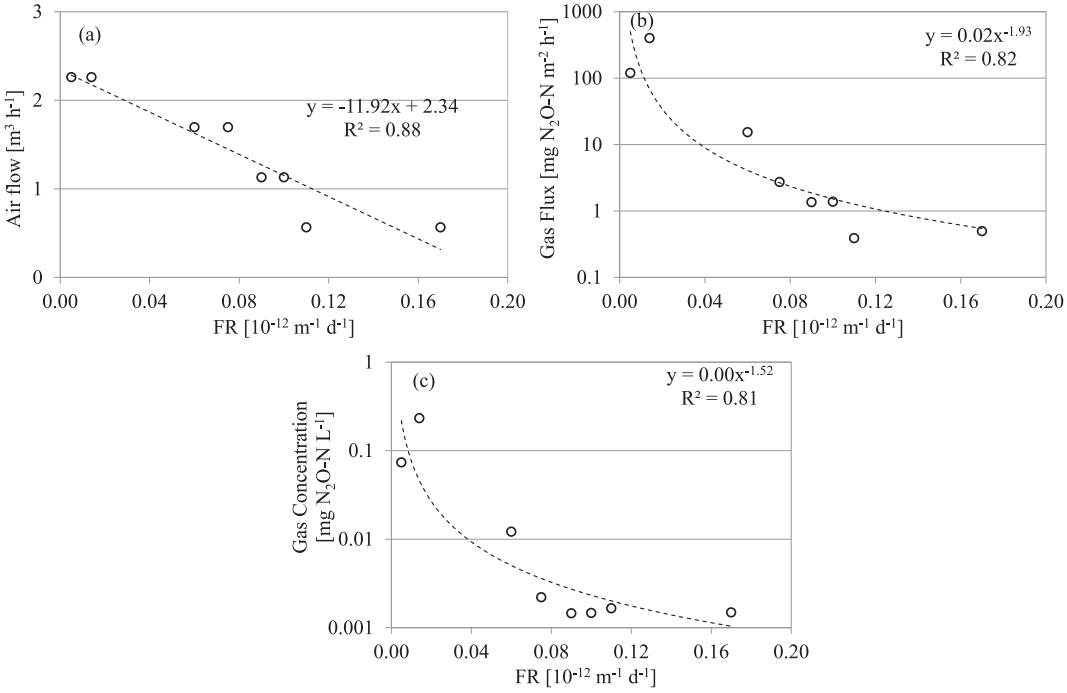

Fig. 4. Relationships between the fouling rate (F_R) and (a): the air flow rate; (b): the N_2O–N gas flux emitted from the MBR tank; (c): the N_2O–N gas concentration of the sample withdrawn from the MBR tank.

pilot plant in view of reducing membrane fouling. However, a detailed analysis of the role of high air flow rate (for fouling mitigation) on the GHG emission has to be performed.

With this in mind, Fig. 4 shows the relationships between the fouling rate (F_R) and the air flow rate (a), the N_2O-N flux emitted from the MBR tank (b) and the N_2O-N concentration of the gas samples withdrawn from the MBR reactor (c).

Data reported in Fig. 4a confirm the decrease of the membrane fouling, in terms of FR, with the increase of air flow, according to a linear relationship (R^2 = 0.88). However, the increase of the air flow rate negatively influences both the N_2O-N gas flux and concentration from the MBR tank. The decrease of the FR, related to the high air flow rate, leads to an increase of both the N_2O-N gas flux and gas concentration of the MBR tank (Fig. 4b-c) according to an exponential relationship. This result is likely due to the increased N_2O stripping effect at high air flow rate. This result is a significant finding for the reduction of the total GHG emission from the pilot plant because the MBR tank produces the 60% (on average) of the total N_2O flux emitted from the pilot plant.

4. Conclusions

The main findings of the study suggest that the increase of the air flow leads to a decrease of the EQI, but increasing the OCs and the indirect emissions, due to the greater power requirement. Direct emissions increase with the air flow rate due to higher N_2O production in denitrification. For fouling control, the best way is to adopt high air flow rates, but increasing significantly the contribution of the MBR tank in producing N_2O. The results of this study can be the basis for mathematical modelling and control of GHG emissions in WWTPs.

Acknowledgements

This work forms part of a research project supported by grant of the Italian Ministry of Education, University and Research (MIUR) through the Research project of national interest PRIN2012 (D.M. 28 dicembre 2012 n. 957/Ric – Prot. 2012PTZAMC) entitled "Energy consumption and GreenHouse Gas (GHG) emissions in the wastewater treatment plants: a decision support system for planning and management – http://ghgfromwwtp.unipa.it" in which the first author of this paper is the Principal Investigator.

Appendix A. Supplementary data

Supplementary data associated with this article can be found, in the online version, at http://dx.doi.org/10.1016/j.biortech.2017.05.043.

References

APHA, 2005. Standard Methods for the Examination of Water and Wastewater. APHA, AWWA and WPCF, Washington DC, USA.

Di Bella, G., Durante, F., Torregrossa, M., Viviani, G., Mercurio, P., Cicala, A., 2007. The role of fouling mechanisms in a membrane bioreactor. Water Sci. Technol. 55 (8–9), 455–464.

Di Bella, G., Di Prima, N., Di Trapani, D., Freni, G., Giustra, M.G., Torregrossa, M., Viviani, G., 2015. Performance of membrane bioreactor (MBR) systems for the treatment of shipboard slops: assessment of hydrocarbon biodegradation and biomass activity under salinity variation. J. Hazard. Mater. 300, 765–778.

Di Trapani, D., Mannina, G., Torregrossa, M., Viviani, G., 2010. Quantification of kinetic parameters for heterotrophic bacteria via respirometry in a hybrid reactor. Water Sci. Technol. 61 (7), 1757–1766.

Di Trapani, D., Di Bella, G., Mannina, G., Torregrossa, M., Viviani, G., 2014. Comparison between moving bed-membrane bioreactor (MB-MBR) and membrane bioreactor (MBR) systems: Influence of wastewater salinity variation. Bioresour. Technol. 162, 60–69.

Fine, P., Hadas, E., 2012. Options to reduce greenhouse gas emissions during wastewater treatment for agricultural use. Sci. Total Environ. 416, 289–299.

Flores-Alsina, X., Arnell, M., Amerlinck, Y., Corominas, L., Gernaey, K.V., Guo, L., et al., 2014. Balancing effluent quality, economic cost and greenhouse gas emissions during the evaluation of (plant-wide) control/operational strategies in WWTPs. Sci. Total Environ. 466–467, 616–624.

Guo, J., Fu, X., Baquero, G.A., Sobhani, R., Nolasco, D.A., Rosso, D., 2016. Trade-off between carbon emission and effluent quality of activated sludge processes under seasonal variations of wastewater temperature and mean cell retention time. Sci. Total Environ. 547, 331–344.

Gupta, D., Singh, S.K., 2012. Greenhouse gas emissions from wastewater treatment plants: a case study of Noida. J. Water Sustain. 2, 131–139.

IPCC. 2007 fourth assessment report: climate change 2007 (AR4). http://www.ipcc.ch/pdf/assessment-report/ar4/wg1/ ar4_wg1_full_report.pdf.
Judd, S., 2011. The MBR Book: Principles and Applications of Membrane Bioreactors in Water and Treatment. Elsevier, Oxford. ISBN: 9781843395188.
Kampschreur, M.J., Temmink, H., Kleerebezem, R., Jetten, M.S.M., van Loosdrecht, M. C.M., 2009. Nitrous oxide emission during wastewater treatment. Water Res. 43, 4093–4103.
Mannina, G., Viviani, G., 2009. Separate and combined sewer systems: A long-term modelling approach. Water Sci. Technol. 60 (3), 555–565.
Mannina, G., Cosenza, A., 2015. Quantifying sensitivity and uncertainty analysis of a new mathematical model for the evaluation of greenhouse gas emissions from membrane bioreactors. J. Membr. Sci. 475, 80–90.
Mannina, G., Trapani, D.D., Viviani, G., Ødegaard, H., 2011. Modelling and dynamic simulation of hybrid moving bed biofilm reactors: Model concepts and application to a pilot plant. Biochem. Eng. J. 56 (1–2), 23–36.
Mannina, G., Ekama, G., Caniani, D., Cosenza, A., Esposito, G., Gori, R., Garrido-Baserba, M., Rosso, D., Olsson, G., 2016a. Greenhouse gases from wastewater treatment – A review of modelling tools. Sci. Total Environ. 551–552, 254–270.
Mannina, G., Morici, C., Cosenza, A., Di Trapani, D., Ødegaard, H., 2016b. Greenhouse gases from sequential batch membrane bioreactors: a pilot plant case study. Biochem. Eng. J. 112, 114–122.
Mannina, G., Cosenza, A., Di Trapani, D., Laudicina, V.A., Morici, C., Ødegaard, H., 2016c. Nitrous oxide emissions in a membrane bioreactor treating saline wastewater contaminated by hydrocarbons. Bioresour. Technol. 219, 289–297.
Mannina, G., Capodici, M., Cosenza, A., Di Trapani, D., Laudicina, V.A., Ødegaard, H., 2017a. Nitrous oxide from moving bed based integrated fixed film activated sludge membrane bioreactors. J. Environ. Manage. 187, 96–102.
Mannina, G., Capodici, M., Cosenza, A., Di Trapani, D., van Loosdrecht, M., 2017b. Nitrous oxide emission in a University of Cape Town membrane bioreactor: the effect of carbon to nitrogen ratio. J. Cleaner. Prod. 149, 180–190.
Mannina, G., Capodici, M., Cosenza, A., Cinà, P., Di Trapani, D., Puglia, A., Ekama, A.G., 2017c. Bacterial community structure and removal performances in IFAS-MBRs: a pilot plant case study. J. Env. Manage. 198, 122–131.
Massara, T.M., Malamis, S., Guisasola, A., Baeza, J.A., Noutsopoulos, C., Katsou, E., 2017. A review on nitrous oxide (N_2O) emissions during biological nutrient removal from municipal wastewater and sludge reject water. Sci. Total Environ. 596–597, 106–123.
Ødegaard, H., 2006. Innovations in wastewater treatment: the moving bed biofilm process. Water. Sci. Technol. 53, 17–33. http://dx.doi.org/10.2166/wst.2006.284.
Otte, S., Grobben, N.G., Robertson, L.A., Jetten, M.S.M., Kuenen, J.G., 1996. Nitrous oxide production by Alcaligenes faecalis under transient and dynamic aerobic and anaerobic conditions. Appl. Environ. Microbiol. 62 (7), 2421–2426.
Sabba, F., Picioreanu, C., Boltz, J.P., Nerenberg, R., 2017. Predicting N_2O emissions from nitrifying and denitrifying biofilms: a modeling study. Water Sci. Technol. 75 (3), 530–538. http://dx.doi.org/10.2166/wst.2016.484.
Singh, R., Hoffman, E.J., Judd, S., 2006. Membranes Technology Ebook. Elsevier, Amsterdam, Netherlands.
Stare, A., Vrecko, D., Hvala, N., Strmcnik, S., 2007. Comparison of control strategies for nitrogen removal in an activated sludge process in terms of operating costs. Water Res. 41 (9), 2004–2014.
Todt, D., Dörsch, P., 2016. Mechanism leading to N_2O production in wastewater treating biofilm systems. Rev. Environ. Sci. Biotechnol. 15 (3), 355–378.